nature geoscience

LETTERS

PUBLISHED ONLINE: 1 FEBRUARY 2009 | DOI: 10.1038/NGEO432

Growth laws for channel networks incised by groundwater flow

Daniel M. Abrams[1], Alexander E. Lobkovsky[1], Alexander P. Petroff[1], Kyle M. Straub[1]*, Brandon McElroy[2], David C. Mohrig[2], Arshad Kudrolli[3] and Daniel H. Rothman[1]†

The re-emergence of groundwater at the surface shapes the Earth's topography through a process known as seepage erosion[1–5]. In combination with flow over land[6], seepage erosion contributes to the initiation and growth of channel networks[1–5]. Seepage processes have also been invoked in the formation of enigmatic amphitheatre-headed channel networks on both Earth[7–11] and Mars[12–14]. However, the role of seepage in producing such channels remains controversial[11,15,16]. One proposed growth law for channel development suggests that the velocity at which channel heads advance is proportional to the flux of groundwater to the heads[17]. Here we use field observations and physical theory to show that this simple model, combined with a second linear response that relates channel branching to the total groundwater flux to the network, is sufficient to characterize key aspects of the growth and form of a kilometre-scale seepage-driven channel network in Florida[18]. We find that the dynamics for the advance of channel heads are reversible, which allows us to estimate the age of the channel network and reconstruct the history of its growth. Our theory also predicts the evolution of the characteristic length scale between channels[19], thereby linking network growth dynamics to geometric form.

Networks of amphitheatre-headed channels known as 'steephead streams'[18] occur abundantly in Liberty County, Florida, east of the Apalachicola River on the Florida panhandle (Fig. 1). The steepheads are incised into 65 m of laterally persistent, medium to coarse, fluviodeltaic and marine sands of Late Pliocene to Pleistocene origin[20], deposited during progradation of the Apalachicola delta[21]. These sands unconformably overlie 15 m of muddy Miocene marine carbonates and sands[20]. Steephead springs occur in the Late Pliocene to Pleistocene sands and examination of the deposit at spring sites reveals no obvious stratigraphic control on their vertical positions[18].

To investigate controls on the horizontal position of springs, we conducted a three-dimensional ground-penetrating radar survey of the water table near a highly bifurcated segment of the channel network (see Supplementary Information). Figure 2a shows that the water table descends as much as 6 m from its highest point midway between channels before reaching the outer contour of the channel network. In general, the height of the water table is a complex function of the spatial distribution of sources (rainfall), sinks (the channel network) and subsurface heterogeneities[22,23]. As rainfall is uniform at this scale, we can test for the influence of heterogeneities by plotting water table height versus the distance to the nearest channel. The good correlation shown in Fig. 2b suggests that distance to the nearest channel, rather than heterogeneities, is the primary determinant of the water table's shape. Consequently the location of springs and the regular structure of this branched drainage network must be a consequence of the intrinsic dynamics of subsurface flow, seepage erosion and sediment transport.

The correlation of Fig. 2b also suggests that the flux of water into any location on the channel network should be proportional to the planform area that is closer to that location than to any other. We call this area the geometric drainage area and plot it in Fig. 3a for each channel tip in the network. Numerical solution of the full three-dimensional hydrodynamic equations for groundwater flow into a periodic array of channels shows that this geometric construction well approximates the relative flux to the tips of channels of varying length (see Supplementary Information).

Howard[17] suggested that the headward erosion rate of a channel tip is proportional to the groundwater flux to the tip. Approximating the flux into the ith tip by the rainfall per unit time into the geometric drainage area a_i associated with that tip then suggests that tip velocity v_i scales as

$$v_i = \beta a_i \tag{1}$$

where β is a transport coefficient (assumed constant) with units $(\mathrm{LT})^{-1}$.

We proceed to test the linear response (1). If it is correct, fast-moving channel tips should be associated with large geometric drainage areas. Figure 3b suggests additionally that larger areas are associated with faster changes in slope as longitudinal valley profiles rise upward from springs towards the relatively flat plain at valley lips. This relation between curvature and area may be understood by assuming that a steady-state longitudinal profile results from a balance between the average erosion rate due to advection and that due to diffusion. Mathematically, this means $\langle v\partial_x h\rangle \sim \langle D\partial^2_{xx} h\rangle$, where h is elevation, D is the topographic diffusivity[24] (assumed constant), v is the horizontal velocity of an elevation contour advancing in the longitudinal direction x, and the angle brackets represent averaging over the upper-slope convexity, which extends a characteristic length r given by its radius of curvature (Fig. 3b). Dimensional analysis of the advection–diffusion balance then yields $v \sim D/r$. Consequently equation (1) predicts that the curvature r^{-1} increases linearly with the geometric drainage area a. Figure 3c tests this prediction for 29 valley heads. The results are indeed consistent with $r^{-1} \simeq \beta a/D$, thereby validating equation (1) and providing an estimate of β/D. Noting that the median radius of curvature is 66 m and assuming

[1]Department of Earth, Atmospheric and Planetary Sciences, Massachusetts Institute of Technology, Cambridge, Massachusetts 02139, USA, [2]Department of Geological Sciences, University of Texas at Austin, Austin, Texas 78712, USA, [3]Department of Physics, Clark University, Worcester, Massachusetts 01610, USA. *Present address: Department of Earth and Environmental Sciences, Tulane University, New Orleans, Louisiana 70118 USA.
†e-mail: dhr@mit.edu.

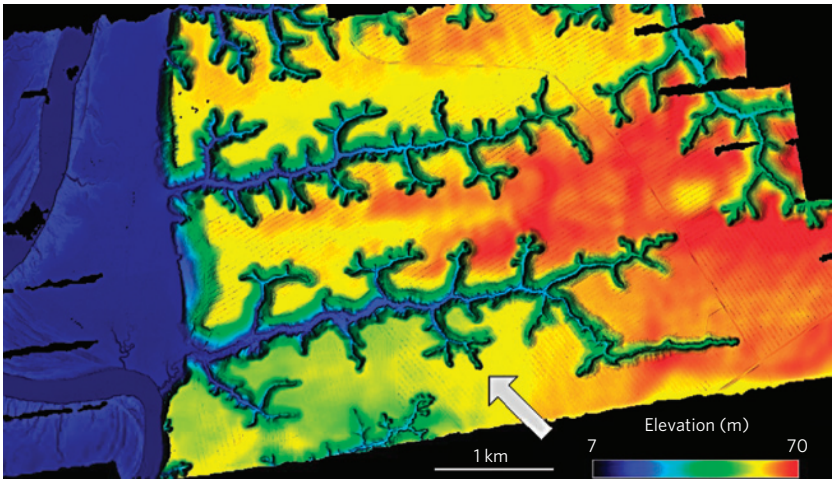

Figure 1 | Topographic map of networks of steephead channels draining into the Apalachicola River, located on the Apalachicola Bluffs and Ravines Preserve, near Bristol, Florida. Topography is shaded with illumination from the east. The arrow points to the location of the water table map in Fig. 2. Mapping data were collected by the National Center for Airborne Laser Mapping. The Universal Transverse Mercator coordinates run from 692000–699000 easting and 3372000–3376000 northing.

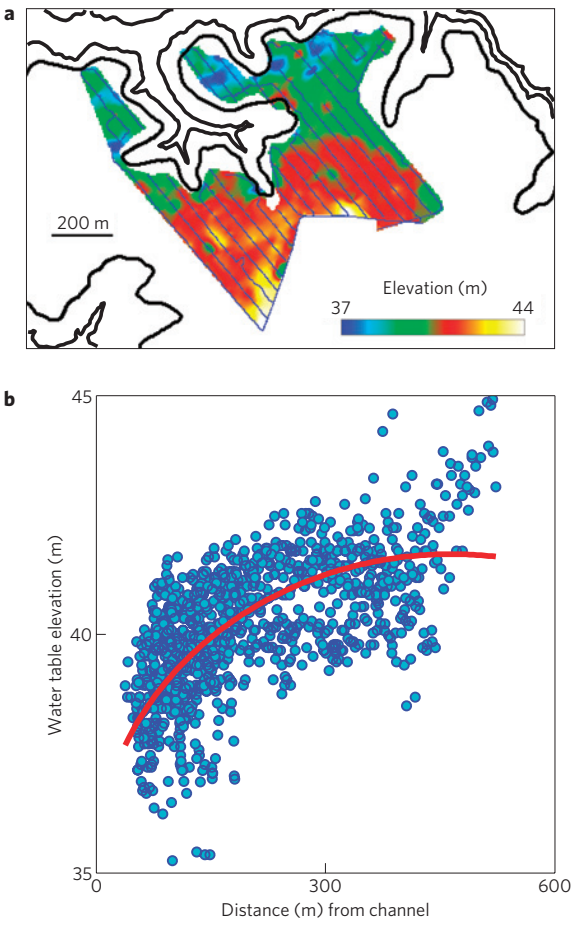

Figure 2 | Water table geometry. a, Elevation of the water table in the region indicated by the arrow in Fig. 1, along with the 35 and 50 m elevation contour of the surface topography (black). The water table was imaged by ground-penetrating radar surveys carried out along transects given by the blue lines. The flat plain away from the channels has a typical elevation of 56 m. **b**, Elevation of the water table plotted against the shortest distance from the 35 m contour. The red curve is the best fitting Dupuit–Forchheimer ellipse[23]. The Spearman rank correlation coefficient $r = 0.69$ ($N = 1{,}065$, $P = 0$). See Supplementary Information.

that the diffusivity $D \simeq 0.02\,\mathrm{m^2\,yr^{-1}}$ (refs 25–28), we find that the headward velocity $v \sim D/r \sim 0.3\,\mathrm{mm\,yr^{-1}}$, consistent with a previous estimate[18].

The water table's shape adjusts continually in response to the advance of channel tips. Given the typical hydraulic conductivity $K \sim 10^{-3}\,\mathrm{m\,s^{-1}}$ for sand[23] and a typical tip area $a \sim 4 \times 10^4\,\mathrm{m^2}$, the timescale for relaxation of the water table is $\sqrt{a}/K \sim 2$ days. Consequently the water table adjusts rapidly—that is, quasistatically—on the timescale of headward growth.

This mundane observation has a profound implication: the headward growth described by equation (1) is reversible. We therefore evolve the network backwards in time by retracting tips i at velocity $-\beta a_i$, continuously updating the a_i values as the network geometry changes. Reversing the process yet again so that time marches forward then provides a reconstruction of the network's growth. Figure 4 shows that new channel tips are generated by both side-branching and tip-splitting events. Computer animation (see Supplementary Information) shows the process dynamically.

An immediate consequence of the reconstruction is an ability to estimate the age of the network. Letting ℓ be the length of a stream and t the time it takes to grow with time-averaged tip velocity $\bar{v}$ and tip area $\bar{a}$, we have

$$t = \frac{\ell}{\bar{v}} = \frac{\ell}{\beta \bar{a}} = \frac{1}{D}\left(\frac{D}{\beta}\right)\left(\frac{\ell}{\bar{a}}\right) \qquad (2)$$

where the second equality follows from averaging equation (1) over time. For the longest channel of the modern network, $\ell \simeq 3.9 \times 10^3$ m and $\bar{a} \simeq 8.3 \times 10^5\,\mathrm{m^2}$. Inserting into equation (2) our previous estimate[25–28] of the diffusivity D and our estimate of D/β from Fig. 3c, we then obtain $t \simeq 0.73$ Myr, roughly accurate within a factor of two, and consistent with the Pliocene–Pleistocene age (~2 Myr) of the sand. These numbers imply that the time-averaged tip velocity is about $5.3\,\mathrm{mm\,yr^{-1}}$. Averaging over all channels for the last 10,000 yr of the network's evolution, however, shows that the current network is growing more slowly, at about $0.5\,\mathrm{mm\,yr^{-1}}$, which represents a refinement of our previous estimate using the curvature–area relation of Fig. 3c.

More fundamentally, the reconstruction also shows an approximate rate law for the generation of new channels by tip-splitting and side-branching. Let $A(t)$ equal the total area drained by the network. Then $\dot{N}/L$ is the production rate, per unit length, of new tips, and A/L is the drainage area, per unit

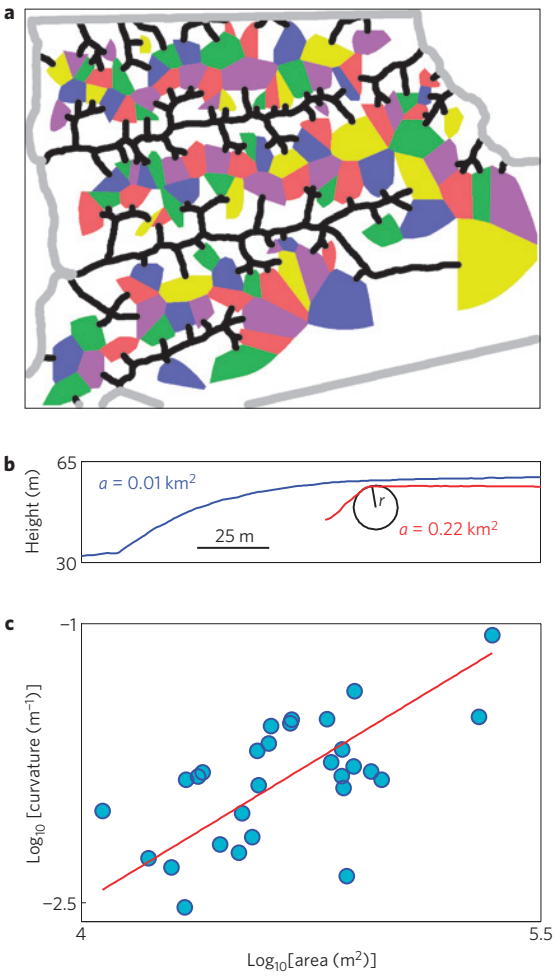

Figure 3 | Geometric drainage areas and the curvature–area relation. **a**, Backbone of the network of Fig. 1 (black) along with the geometric drainage area a (coloured polygons) associated with each channel tip. Grey lines indicate boundaries used to delineate the overall basin. **b**, Longitudinal valley profiles associated with small (0.01 km^2) and large (0.22 km^2) geometric drainage areas. In the latter case, the radius of curvature, r, of the upper-slope convexity is indicated. Horizontal axis is only for scale. Profiles rise upward from springs and terminate at the flat plain. **c**, Log–log plot of the curvature r^{-1} versus geometric area a for isolated non-bifurcating valley heads. The Pearson correlation coefficient $r = 0.62$ ($N = 29$, $P < 0.001$). The straight line is the best fit to $r^{-1} = (\beta/D)a$, providing the estimate $\beta/D = 3.2 \pm 0.7 \times 10^{-7}$ m^{-3}. The valley profiles of **b** correspond to the smallest and largest areas in **c**. See Supplementary Information.

length, into the entire network. The generation of new channel tips must ultimately derive from a three-dimensional erosional instability[1–5,29,30]. We know of no theory for this instability, but the mechanism that drives it must be drainage into the network. Consequently we expect that A/L is proportional to a force density that creates new tips at rate $\dot{N}/L$ per unit length. Hypothesizing a linear response, we obtain

$$\frac{\mathrm{d}N}{\mathrm{d}t} = \alpha A \tag{3}$$

where α is a rate constant per unit area, with units $(\mathrm{L}^2\mathrm{T})^{-1}$. We test the integral form of equation (3) by plotting $N(t)$, the number of channel tips, versus $\int_0^t A(t')\,\mathrm{d}t'$. The result, shown in the inset of Fig. 4, is consistent with the linear response equation (3); the slope gives the rate constant α.

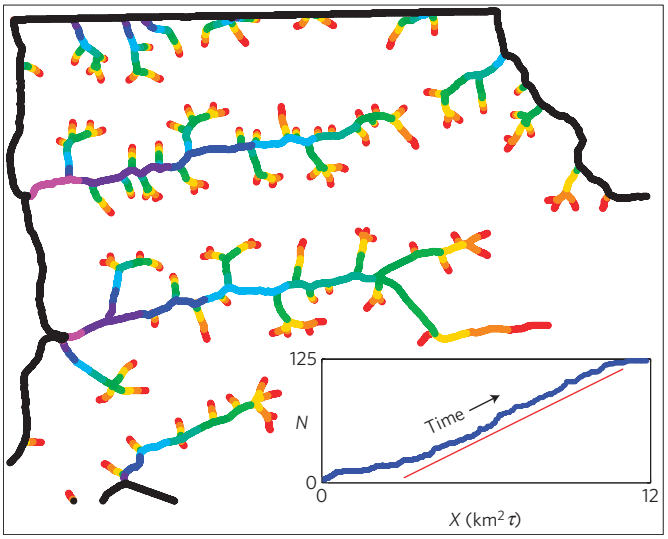

Figure 4 | Reconstruction of network growth. Each coloured segment corresponds to one-tenth of the elapsed time of growth. Black segments represent initial conditions. Computer animations are available in Supplementary Information. Inset: Plot of the number of reconstructed channel tips, N, versus $X = \int_0^\tau A(\tau')\mathrm{d}\tau'$, where $\tau = t/t_{\max}$. After an initial transient the growth is approximately linear, thereby validating equation (3).

The linear response relations (1) and (3) provide, respectively, the growth and birth rates of channels. The ratio of the transport coefficient β to the rate constant α is a length scale that represents the characteristic growth of the network's total length L during the characteristic time between the birth of new channels. We can obtain β/α explicitly by noting from equation (1) that $\dot{L} = \beta \sum_i a_i$ and integrating to obtain $\beta t = L/\sum_i \bar{a}_i$. On the other hand, integration of equation (3) yields $\alpha t = N/\bar{A}$, where $\bar{A}$ is the time-averaged area draining into the entire network. Then

$$\frac{\beta}{\alpha} = \frac{L(t)}{N(t)}\left(\frac{\bar{A}(t)}{\sum_i \bar{a}_i(t)}\right) \tag{4}$$

Note that all terms on the right-hand side depend on time, but the left-hand side does not. Thus, lengths, areas and the number of channels must evolve such that β/α is constant. Our reconstruction confirms this prediction: over the last half of the network's growth, $\beta/\alpha \simeq 461$ m with a root-mean square fluctuation of less than 3%.

To further understand the length scale β/α, we define the dimensionless 'screening efficiency' $S = \sum_i \bar{a}_i/\bar{A}$. Substitution into equation (4) and rearranging then yields

$$L = \left(\frac{\beta}{\alpha}\right) SN \tag{5}$$

The screening efficiency $0 \le S \le 1$ is the fractional extent to which tips draw groundwater away from channel sidewalls. In the limit in which all groundwater flows to tips, $S = 1$ and each tip contributes a length β/α to the total channel length L, consistent with our dimensional argument. Less efficient screening ($S < 1$) implies less length per tip. (Here we find $S = 0.59 \pm 0.01$ while $\beta/\alpha \simeq$ const.) But the fundamental length scale that must determine all other lengths is β/α.

Foremost among network length scales is the average distance A/L between any point on the network and the closest groundwater divide. This 'dissection' scale[19] is the inverse of Horton's drainage density[6] L/A. It is typically studied in the context of mature, static networks in which the tips no longer gather sufficient water to

grow[19]. Here we instead provide a dynamic view. Dividing both sides of equation (5) by A, it can be seen immediately that the drainage density increases as the number N of tips grows.

Decades ago, Dunne[1,3,4] advanced a conceptual model for the development of seepage-driven networks. Its principal components—headward growth due to groundwater focusing and generation of new channel heads by tip-splitting and side-branching—are encoded here in terms of two linear response relations. After validating these linear laws by analysis of the Florida network's present and past development, we find that the evolution of lengths, drainage density and number of tips is slaved to the transport coefficient β and rate constant α that set the respective timescales for the network's growth and ramification. This result provides an explicit link between the dynamics of a network and its static structure. Although this link does not by itself provide an immediate method for resolving the mysterious provenance of other amphitheatre-headed channels[7–16], we expect that the growth laws on which it is based will be useful for understanding the mechanisms that produce such shapes in addition to providing further reconstructions of past network growth.

Received 21 August 2008; accepted 9 January 2009; published online 1 February 2009

References

1. Dunne, T. *Runoff Production in a Humid Area*. Thesis (Johns Hopkins Univ., 1969). Also published as US Department of Agriculture Report ARS 41–160 (1970).
2. Dunne, T. in *Hillslope Hydrology* (ed. Kirkby, M. J.) 227–293 (Wiley, 1978).
3. Dunne, T. Formation and controls of channel networks. *Prog. Phys. Geogr.* **4**, 211–239 (1980).
4. Dunne, T. in *Groundwater Geomorphology: The Role of Subsurface Water in Earth-Surface Processes and Landforms* Vol. 252 (eds Higgins, C. G. & Coates, D. R.) 1–28 (Geol. Soc. Am. Special Paper, Geological Society of America, 1990).
5. Dietrich, W. E. & Dunne, T. in *Channel Network Hydrology* (eds Beven, K. & Kirby, M. J.) 175–219 (Wiley, 1993).
6. Horton, R. E. Erosional development of streams and their drainage basins: Hydrophysical approach to quantitative morphology. *Geol. Soc. Am. Bull.* **56**, 275–370 (1945).
7. Wentworth, C. K. Principles of stream erosion in Hawaii. *J. Geol.* **36**, 385–410 (1928).
8. Laity, J. E. & Malin, M. C. Sapping processes and the development of theater-headed valley networks on the Colorado plateau. *Geol. Soc. Am. Bull.* **96**, 203–17 (1985).
9. Orange, D. L., Anderson, R. S. & Breen, N. A. Regular canyon spacing in the submarine environment: The link between hydrology and geomorphology. *GSA Today* **4**, 1–39 (1994).
10. Schorghofer, N., Jensen, B., Kudrolli, A. & Rothman, D. H. Spontaneous channelization in permeable ground: Theory, experiment, and observation. *J. Fluid Mech.* **503**, 357–374 (2004).
11. Lamb, M. P. *et al*. Can springs cut canyons into rock? *J. Geophys. Res.* **111**, E07002 (2006).
12. Higgins, C. G. Drainage systems developed by sapping on Earth and Mars. *Geology* **10**, 147–152 (1982).
13. Malin, M. C. & Carr, M. H. Groundwater formation of martian valleys. *Nature* **397**, 589–591 (1999).
14. Malin, M. C. & Edgett, K. Evidence for recent groundwater seepage and surface runoff on Mars. *Science* **288**, 2330–2335 (2000).
15. Lamb, M. P., Howard, A. D., Dietrich, W. E. & Perron, J. T. Formation of amphitheater-headed valleys by waterfall erosion after large-scale slumping on Hawaii. *GSA Bull.* **19**, 805–822 (2007).
16. Lamb, M. P., Dietrich, W. E., Aciego, S. M., DePaolo, D. J. & Manga, M. Formation of Box Canyon, Idaho, by megaflood: Implications for seepage erosion on Earth and Mars. *Science* **320**, 1067–1070 (2008).
17. Howard, A. D. in *Sapping Features of the Colorado Plateau: A Comparative Planetary Geology Field Guide* (eds Howard, A. D., Kochel, R. C. & Holt, H. E.) 71–83 (NASA Scientific and Technical Information Division, 1988).
18. Schumm, S. A., Boyd, K. F., Wolff, C. G. & Spitz, W. J. A ground-water sapping landscape in the Florida Panhandle. *Geomophology* **12**, 281–297 (1995).
19. Montgomery, D. R. & Dietrich, W. E. Channel initiation and the problem of landscape scale. *Science* **255**, 826–830 (1992).
20. Schmidt, W. *Alum Bluff, Liberty County, Florida*. Open File Report 9 (Florida Geological Survey, 1985).
21. Rupert, F. R. *The Geomorphology and Geology of Liberty County, Florida*. Open File Report 43 (Florida Geological Survey, 1991).
22. Polubarinova-Kochina, P. I. A. *Theory of Ground Water Movement* (Princeton Univ. Press, 1962).
23. Bear, J. *Dynamics of Fluids in Porous Media* (Dover, 1972).
24. Culling, W. E. H. Analytic theory of erosion. *J. Geol.* **68**, 336–344 (1960).
25. McKean, J. A., Dietrich, W. E., Finkel, R. C., Southon, J. R. & Caffee, M. W. Quantification of soil production and downslope creep rates from cosmogenic ^{10}Be accumulations on a hillsope profile. *Geology* **21**, 343–346 (1993).
26. Rosenbloom, N. A. & Anderson, R. S. Hillslope and channel evolution in a marine terraced landscape, Santa Cruz, California. *J. Geophys. Res.* **99**, 14013–14029 (1994).
27. Fernandes, N. F. & Dietrich, W. E. Hillslope evolution by diffusive processes: The timescale for equilibrium adjustments. *Wat. Resour. Res.* **33**, 1307–1318 (1997).
28. Small, E. E., Anderson, R. S. & Hancock, G. S. Estimates of the rate of regolith production using ^{10}Be and ^{26}Al from an alpine hillslope. *Geomorphology* **27**, 131–150 (1999).
29. Howard, A. D. & McLane, C. F. Erosion of cohesionless sediment by groundwater seepage. *Wat. Resour. Res.* **24**, 1659–1674 (1988).
30. Lobkovsky, A. E., Jensen, B., Kudrolli, A. & Rothman, D. H. Threshold phenomena in erosion driven by subsurface flow. *J. Geophys. Res.-Earth* **109**, F04010 (2004).

Acknowledgements

We would like to thank The Nature Conservancy for access to the Apalachicola Bluffs and Ravines Preserve, and K. Flournoy, B. Kreiter, S. Herrington and D. Printiss for guidance on the Preserve. We would also like to thank D. Forney, D. Jerolmack and J. T. Perron for helpful suggestions and assistance in the field, and T. Dunne and J. T. Perron for critical reviews of the manuscript. This work was supported by Department of Energy Grants FG02-99ER15004 and FG02-02ER15367. D.H.R. also thanks the Radcliffe Institute for Advanced Study for providing a year-long fellowship during which much of this work was completed.

Author contributions

D.M.A., A.E.L., A.P.P., K.M.S. and D.H.R. contributed equally to this work. D.M.A., A.E.L., A.P.P. and D.H.R. developed theory and carried out field work and data analysis. K.M.S. and A.K. carried out field work and data analysis. B.M. and D.C.M. carried out field work and analysed regional sedimentology. D.H.R. wrote the paper, with input from D.M.A., A.E.L., A.P.P., K.M.S. and B.M.

Additional information

Supplementary Information accompanies this paper on www.nature.com/naturegeoscience. Reprints and permissions information is available online at http://npg.nature.com/reprintsandpermissions. Correspondence and requests for materials should be addressed to D.H.R.